J. Astrophys. Astr. (2009) **30,** 165–175

Rapid Neutron Capture Process in Supernovae and Chemical Element Formation

Rulee Baruah[1,*], Kalpana Duorah[2] & H. L. Duorah[2]
[1]*Department of Physics, HRH The Prince of Wales Institute of Engineering and Technology, Jorhat 785 001, India.*
[2]*Department of Physics, Gauhati University, Guwahati 781 014, India.*
[*]*e-mail: ruleebaruah@yahoo.co.in*

Received 2007 May 28; accepted 2009 September 29

Abstract. The rapid neutron capture process (r-process) is one of the major nucleosynthesis processes responsible for the synthesis of heavy nuclei beyond iron. Isotopes beyond Fe are most exclusively formed in neutron capture processes and more heavier ones are produced by the r-process. Approximately half of the heavy elements with mass number $A \succ 70$ and all of the actinides in the solar system are believed to have been produced in the r-process. We have studied the r-process in supernovae for the production of heavy elements beyond $A = 40$ with the newest mass values available. The supernova envelopes at a temperature $\succ 10^9$ K and neutron density of 10^{24} cm^{-3} are considered to be one of the most potential sites for the r-process. The primary goal of the r-process calculations is to fit the global abundance curve for solar system r-process isotopes by varying time dependent parameters such as temperature and neutron density. This method aims at comparing the calculated abundances of the stable isotopes with observation. We have studied the r-process path corresponding to temperatures ranging from 1.0×10^9 K to 3.0×10^9 K and neutron density ranging from 10^{20} cm^{-3} to 10^{30} cm^{-3}. With temperature and density conditions of 3.0×10^9 K and 10^{20} cm^{-3} a nucleus of mass 273 was theoretically found corresponding to atomic number 115. The elements obtained along the r-process path are compared with the observed data at all the above temperature and density range.

Key words. Supernova—nucleosynthesis—abundance—r-process.

1. Introduction

Burbidge *et al.* (1957), in their seminal paper, outlined the rapid neutron capture process in the supernova envelope at a high neutron density and a temperature of 10^9 degrees. According to them, this mode of synthesis is responsible for the production of a large number of isotopes in the range $70 \leq A \leq 209$, and also for synthesis of uranium and thorium. This would explain the abundances of the neutron rich nuclei in the periodic table. Major advances have been made in calculating r-process nucleosynthesis in supernovae (Woosley *et al.* 1992) and in using a wide range of

model parameters to obtain yields that approximate the solar r-process abundances (Kratz *et al.* 1993). Studies of galactic chemical evolution (Mathews & Cowan 1992) show that the enrichment of the r-process elements in the galaxy is consistent with low mass type II supernovae being the r-process sites. In the usual picture the r-process stops when the neutron supply ceases (freeze-out). The produced very neutron rich progenitor nuclei then undergo a series of β-decays until they reach a stable nucleus whose calculated abundance can then be compared with observation. It was recognised that the extremely high neutron densities and temperatures needed were probably attainable only in dynamical events, i.e., supernovae.

The essential feature of the r-process is that a large flux of neutrons becomes available in a short time interval for addition to elements of the iron group, or perhaps, in cases where the abundances in the iron group are abnormally small, for addition to light nuclei such as Ne^{22}. So we started our analysis with $A = 40$ and obtained the abundances beyond that. We have summarised our calculations within a site-independent, classical approach based on neutron number density n_n and temperature T_9, defining the neutron binding (separation) energy Q_n of the path, where the waiting point approximation, i.e., (n, γ) $\leftrightarrow$ (γ, n) equilibrium could be applied. The dependence on nuclear masses enters via Q_n.

We choose supernova as the site for r-process because the supernova light curves show the presence of ${}_{98}Cf^{254}$. We have considered the r-process in supernovae for the production of heavy elements, under extreme conditions of temperature and density. For our purpose, the most interesting evolution occurs as the temperature falls from 10^{10} K to 10^9 K. Beginning at about 10^{10} K, nuclear statistical equilibrium (NSE) favours the assemblage of nucleons into α-particles and heavy nuclei. As the temperature drops below about 5.0×10^9 K, the reactions responsible for converting α-particles back into heavy nuclei begin to fall out of equilibrium. By 3.0×10^9 K, the charged particle reactions freeze out. Below this temperature, the r-process occurs until the temperature reaches (1–2) $\times 10^9$ K, where the neutron reactions also cease as the neutrons are depleted (Woosley *et al.* 1994). Using new mass tables of Audi *et al.* (2003) we have calculated the average excess neutron binding energy to nuclei with neutron number which is then used in the calculation of neutron capture chain. We start with a temperature of 1.0×10^9 K and neutron number density of 10^{20} cm^{-3} as these are the conditions prevailing in supernova envelopes during the eventually expanding stages. In our present paper, we emphasize only on the r-process path to obtain the elements in our astrophysical conditions considered and consequent build-up to heavier nuclei. In our next paper, we propose to present the abundances of these elements along the path.

2. Source of neutron flux

For the r-process nucleosynthesis in supernovae, the existence of enormous neutron flux is necessitated. Normal stellar matter has a neutron/proton ratio near unity making it virtually impossible to free sufficient neutrons relative to seed nuclei. Reactions such as $^{13}C(\alpha, n)^{16}O$ can produce free neutrons in red giants, but the number of these free neutrons is also small. It is possible to circumvent this problem by having the only charged particles accompanying the neutrons be alphas. Single alpha particles do not capture neutrons. It is proposed that (Schramm 1973) at high temperatures associated with the collapse of massive iron core in type II supernovae, iron will photo-dissociate

into alphas and neutrons as:

$$^{56}\mathrm{Fe} \rightarrow 13\alpha + 4n.$$

As the material expands and cools from these photo-dissociation conditions, the alphas recombine again to produce heavy iron peak nuclei. However, these recombination is hampered by the fact that alphas only systhesize heavy elements via three-body interactions. Thus there will be a time during which a few iron peak seed nuclei have been produced in a sea of alphas and neutrons. The ratio of neutrons to seed will be large, so that an r-process can take place.

Another set of conditions where large number of free neutrons exist is when the temperature and density get sufficiently high that the reaction $\mathrm{p} + \mathrm{e}^- \rightarrow \mathrm{n} + \nu_e$ dominates over $\mathrm{n} + \mathrm{e}^+ \rightarrow \mathrm{p} + \bar{\nu}_e$ (Arnett 1979). Thus neutronisation refers to electron capture driven by high electron Fermi energy (i.e., high density). Subsequently, $\mathrm{p} + \mathrm{e}^- \rightarrow \mathrm{n} + \nu_e$ at high density. Moreover, nuclei resist electron capture because of the large threshold energies required as they become more neutron rich. Also electron capture on free protons is limited by the small abundance of free protons. These problems are eased by higher density and higher temperature, so neutronization speeds up as collapse continues. Once collapse begins, neutronization becomes the dominant mode of neutrino productions, overwhelming thermal processes.

According to Mukhopadhyay (2007), the neutrino–antinutrino oscillation under gravity explains the source of abnormally large neutron abundance to support the r-process nucleosynthesis in astrophysical site, e.g., supernova. He also proposed two related reactions

$$\mathrm{n} + \nu_e \rightarrow \mathrm{p} + \mathrm{e}^-; \quad \mathrm{p} + \bar{\nu}_e \rightarrow \mathrm{n} + \mathrm{e}^+$$

as given by Arnett (1979). If $\bar{\nu}_e$ is over-abundant than ν_e, then, from this expression, neutron production is expected to be more than proton production into the system. Therefore, the possible conversion of ν to $\bar{\nu}_e$ due to gravity induced oscillation explains the over-abundance of neutron.

In the build-up of nuclei by the r-process, the reactions which govern both the rate of flow and the track followed in the (A, Z) plane are the (n, γ) and (γ, n) reactions, beta decay and at the end of the track the neutron induced fission. The timescale τ_n for a heavy nucleus to capture an additional neutron is rapid on the competing timescale τ_β for it to undergo beta decay. Whereas τ_β depends only on nuclear species, τ_n depends critically on the ambient neutron flux.

$$\lambda_n > \lambda_\beta (\tau_n < \tau_\beta). \tag{1}$$

In rapid process, a sufficient flux of neutrons makes τ_n much shorter than τ_β. Then neutron capture will proceed into the very neutron rich and unstable regions far from the valley of beta stability. Once the neutron flux is exhausted, the unstable nuclei produced by the r-process will beta decay to the valley of stability to form the stable r-process elements.

3. Nuclear physics considerations and the r-process path

To illustrate the significant differences of the astrophysical conditions during the r-processing, we refer to the classical quantity, namely, the neutron binding

(separation S_n) energy Q_n, that represents the r-process path in the chart of nuclides once the specific values of neutron density n_n and the temperature T are assigned. The Q_n values vary in time as well as in space along with the dynamical evolution of our astrophysical environment.

3.1 *Dynamical evolution of the neutrino heating phase in type-II supernovae*

We first summarize the type-II supernova explosion scenario according to the current understanding. We emphasize some characteristic features on the hydrodynamical evolution of the neutrino wind phase. During the final stages of the evolution of a massive ($8 \sim 25\,M_\odot$) star, an 'iron' core forms in its central region and subsequently undergoes gravitational collapse. When the central density reaches nuclear matter density, the collapse stops abruptly to cause a 'core bounce'. A hydrodynamical shock wave is created and starts to propagate outward. According to calculations (Bruenn 1989a), this shock wave loses its entire kinetic energy within a few milliseconds to stall well inside the outer edge of the initial iron core, and no immediate disruption (the 'prompt' expolsion) of the star occurs. On a timescale from several tens of milliseconds to about half a second, the neutrinos streaming out from the new born neutron star can deposit energy behind the standing accretion shock at high enough a rate to revive its outward motion and initiate the final explosion of the star. This is the neutrino-driven 'delayed' explosion mechanism originally suggested by Wilson *et al.* (1986).

The neutron star releases its gravitational binding energy of several 10^{53} erg in the form of neutrino radiation. A region of net energy deposition by neutrinos ('neutrino heating') naturally emerges at the periphery of the neutron star because of the decrease of temperature with increasing radius. The energy is transferred to the stellar gas predominently by absorption of electron neutrinos (ν_e) on neutrons and electron anti-neutrinos ($\bar{\nu}_e$) on protons. About one percent of the neutron star's binding energy is sufficient to drive a powerful shock into the overlaying stellar mantle. Behind the shock, an extended and rapidly expanding region of low density and relatively high temperature develops and is further energized by neutrino heating.

Janka (1993) performed hydrodynamical simulations of the formation and evolution of the neutrino-wind phase of a type II supernova with a proper description of the neutrino physics and an adequate representation of the equation of state. The hydrodynamical investigations were carried on from an initial configuration made available by Wilson. From Wilson's post-collapse model the radial profiles of density, temperature, electron concentration, composition and velocity were taken to specify the initial conditions for the set of partial differential equations, which was integrated in time to follow the gas composition and the evolution of the fluid flow in spherical symmetry. The equation of state for the stellar gas contained the contributions from nucleus, α-particles, and a representative typical heavy nucleus in nuclear statistical equilibrium. The model evolved under the influence of the neutrino fluxes from the protoneutron star at the center. Since all hydrodynamical and thermodynamical quantities were determined from the numerically solved set of equations, the effects of the particular choice of the initial model configuration were not crucial and became even less relevant as time went on. The most important parameter of the input model to influence the simulated evolution was the mass of the central neutron star (Witti *et al.* 1994). However, the hydrodynamical evolution in the range of temperatures below $T_9 = 2$ is not very fast (Takahashi *et al.* 1994).

3.2 *The r-process network and the waiting-point approximation*

Supernova is a dynamical event. When a constant S_n (n_n and T) is assumed over a duration time τ, then the nuclei will still be existent in the form of highly unstable isotopes, which have to decay back to β-stability. In reality n_n and T will be time dependent. As long as these are high enough to ensure the waiting point approximation, the system will immediately adjust to the new equilibrium and only the new S_n (n_n and T) is important. The abundance flow from each isotopic chain to the next is governed by beta decays. The waiting point approximation is only valid for high temperatures and neutron number densities of the gas. If not, the flow of nuclei towards higher neutron number N for a given proton number Z is steadily depleted by beta decay. As a result only a small fraction of the flow can easily reach a waiting point. Cameron *et al.* (1983b) found that for temperatures of 2.0×10^9 K and higher, the waiting point approximation was valid for neutron number densities as low as 10^{20} cm^{-3}. For lower temperature ($T < 10^9$ K) even with high values of $n_n \approx 10^{25}$ cm^{-3}, the waiting point approximation is not valid. The r-process path requires a synthesis time of the order of seconds to form the heaviest elements such as thorium, plutonium and uranium.

The r-process network includes radiative neutron capture, i.e., (n, γ) reactions, the inverse photo-disintegration, i.e., (γ, n) reactions, β-decay, i.e., (β, γ) processes and β-delayed neutron emission, i.e., (β, n) processes. If the neutron density is very high, successive (n, γ) reactions may produce very neutron rich isotopes out of the limited α-process network in a 'mini r-process'. The (n, γ) and (γ, n) reactions are then much faster than β-decays. Therefore, as soon as the 'proper' r-process is started, the isotopic abundances, stuck at the most neutron-rich isotopes included in the α-process network, will quickly be redistributed according to the (n, γ) $\leftrightarrow$ (γ, n) equilibrium (Takahashi *et al.* 1994). In our model, the neutron number densities are so high that an equilibrium between the (n, γ) and (γ, n) reactions is quickly established.

In an (n, γ) $\leftrightarrow$ (γ, n) equilibrium (the waiting-point approximation), the maximum abundances in isotopic chains occur at the same neutron separation energy, which is determined by a combination of n_n and T_9 in an astrophysical environment. Connecting the abundance maxima in isotopic chains defines the so called r-process path. The build-up of heavy nuclei is governed by the abundance distribution in each isotopic chain from (n, γ) $\leftrightarrow$ (γ, n) equilibrium and by effective decay rates λ_β^Z of isotopic chains. After charged particle freeze-out, when only (n, γ) $\leftrightarrow$ (γ, n) equilibrium remain in place, matter can progress to heavier nuclei via β-decays between isotopic chains, which is modelled by the r-process network to follow further evolution (Freiburghaus *et al.* 1999).

4. Calculation of the r-process path

A nucleus of fixed Z cannot add neutrons infinitely even in the presence of an intense neutron flux. The binding energy of each successive neutron becomes progressively weaker as more and more neutrons are added until ultimately the binding falls to zero, which sets an upper limit to neutron addition at fixed Z. The nucleus then waits until β-decay allows it to move onto the next nucleus. Thus in a rapid process two inverse reactions $\mathrm{n} + (Z, A) \leftrightarrow (Z, A+1) + \gamma$ come to an equilibrium. This balance governs the equilibrium distribution of isotope abundances for a given Z. The maximum abundance along an isotope chain is determined by the temperature and neutron density.

Given that $A/(A+1) \approx 1$, the abundance maxima in each isotopic chain are determined by the neutron number density n_n and temperature T. The maximum value of the abundance occurs at neutron separation energy S_n which is same for all isotopic chains irrespective of Z. Approximating abundances $Y(Z, A+1)/Y(Z, A) \approx 1$ at the maximum and keeping all other quantities constant, the neutron separation energy S_n has to be the same for the abundance maxima in all isotopic chains.

The condition for the dynamical equilibrium between (n, γ) and (γ, n) reactions for nucleus $X(A, Z)$ is expressed as (Burbidge *et al.* 1957):

$$X(A, Z) + n \Longleftrightarrow X(A+1, Z) + \gamma + Q_n(A, Z), \tag{2}$$

where $Q_n(A, Z)$ is the neutron binding (separation energy S_n) to the nucleus $X(A, Z)$. Writing $n(A, Z)$ and n_n for the number densities of the nuclei (A, Z) and neutrons respectively, the statistical balance in this reaction is expressed by (Burbidge *et al.* 1957):

$$\log(n(A+1, Z)/n(A, Z)) = \log\ n_n - 34.07 - (3/2)\log\ T_9 + (5.04/T_9)Q_n \tag{3}$$

T_9 being temperature in units of 10^9 degrees.

Using the condition that in equilibrium, $n(A+1, Z) \approx n(A, Z)$ we obtain Q_n as:

$$Q_n = (T_9/5.04)(34.07 + (3/2)\log\ T_9 - \log\ n_n). \tag{4}$$

A rough estimate of Q_n values that are preferred for explaining the r-process abundance curve can be gained by taking into account the correlation between the r-process abundance peaks and the neutron magic numbers. The prominent peaks at $A \approx 130$ and $A \approx 195$ are correlated with the nuclear shell effects of their precursor nuclei near the neutron magic numbers 82 and 126 respectively. With the aid of nuclear mass formula, one finds from the abundance peaks that the Q_n value is most likely somewhere in between 2 and 4 MeV. To attain this, we take the temperature and density conditions considered here to range from

$$T = 1.0 \times 10^9\,\mathrm{K} \text{ to } 3.0 \times 10^9\,\mathrm{K} \quad \text{and} \quad n_n = 10^{20}\,\mathrm{cm}^{-3} \text{ to } 10^{30}\,\mathrm{cm}^{-3}.$$

The variation of Q_n values with temperature and neutron number densities is shown in Table 1.

We then tried to outline a method of calculation of r-process abundances which may eventually be capable of yielding a theoretical abundance curve on the basis of nuclear data alone. First, we consider the determination of $Q_n(A, Z)$ on the basis of smooth Weizsacker atomic mass formula given by equation (5) neglecting shell, pairing and quadrupole deformation effects:

$$\begin{aligned} M_w(A, Z) = (A-Z)M_n + ZM_p - (1/c^2)[\alpha A - \beta(A-2Z)^2/A \\ - \gamma A^{2/3} - \epsilon Z(Z-1)/A^{1/3}], \end{aligned} \tag{5}$$

where M_n and M_p are masses of the neutron and proton and α, β, γ and ϵ are constants in energy units, which represent volume, isotopic, surface and coulomb energy parameters respectively, the values being taken from Burbidge *et al.* (1957). With these we modify the expression for $M(A, Z)$ as:

$$M(A, Z) = M_w(A, Z) - (1/c^2)[f(N) + g(Z)], \tag{6}$$

Table 1. Variation of Q_n values with temperature and density.

T_9(K)	n_n(cm^{-3})	Q_n(Mev)	T_9(K)	n_n(cm^{-3})	Q_n(Mev)
1.0	10^{20}	2.79	1.0	10^{22}	2.39
1.2	10^{20}	3.37	1.2	10^{22}	2.90
1.4	10^{20}	3.96	1.4	10^{22}	3.41
1.6	10^{22}	4.56	1.6	10^{22}	3.93
1.0	10^{24}	1.99	1.8	10^{22}	4.45
1.2	10^{24}	2.41	1.2	10^{26}	1.95
1.4	10^{24}	2.85	1.4	10^{26}	2.30
1.6	10^{24}	3.29	1.6	10^{26}	2.65
1.8	10^{24}	3.73	1.8	10^{26}	3.01
2.0	10^{24}	4.17	2.0	10^{26}	3.38
1.6	10^{28}	2.02	2.2	10^{26}	3.74
1.8	10^{28}	2.30	2.4	10^{26}	4.11
2.0	10^{28}	2.58	2.2	10^{30}	1.98
2.2	10^{28}	2.87	2.4	10^{30}	2.19
2.4	10^{28}	3.16	2.6	10^{30}	2.42
2.6	10^{28}	3.45	2.8	10^{30}	2.63
2.8	10^{28}	3.74	3.0	10^{30}	2.84
3.0	10^{28}	4.03			

where $M_w(A, Z)$ represents the Weizsacker expression given by equation (5). With this we calculate the neutron binding energy as:

$$Q_n(A, Z) = B_n(A + 1, Z) = c^2[M(A, Z) + M_n - M(A + 1, Z)]. \tag{7}$$

We note that Q_n for nucleus (A, Z) is equal for the neutron binding energy B_n (taken positive) in nucleus $(A + 1, Z)$. These functions of N and Z separately takes into account the important effects on nuclear masses of:

- neutron and proton shell structure
- spheroidal quadrupole deformation of partially filled shells and
- pairing of neutrons and pairing of protons.

The quantities $f(N)$ and $g(Z)$ will be discontinuous functions at magic closed shell numbers for N and Z respectively. The sign is taken negative so that $f(N)$ and $g(Z)$ as positive quantities, decrease the mass and add to the stability of the nucleus.

We now obtain:

$$Q_n(A, Z) = f(A, Z) + f'(A - Z) \tag{8}$$

putting $M(A, Z)$ from equation (6) and using:

$$f'(A - Z) = f'(N) = df(N)/d(N) = f(A + 1 - Z) - f(A - Z). \tag{9}$$

On simplification and on putting $Z = A - N$, we rewrite equation (8) as:

$$Q_n(A, N) = f(A, N) + f'(N).$$

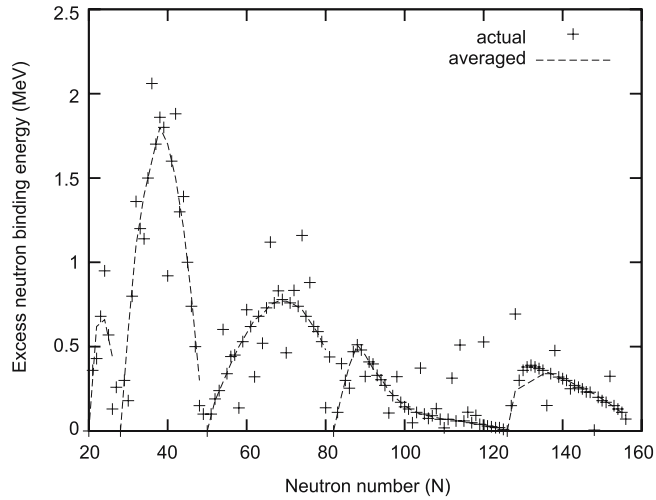

Figure 1. The average excess neutron binding energy *vs.* neutron number N, over that given by the smooth Weizsacker atomic mass formula.

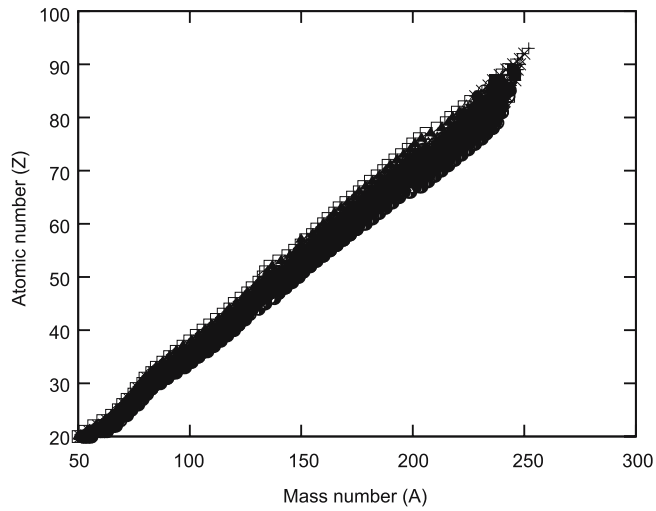

Figure 2. The average r-process path in the (A, Z) plane at all the temperature and density conditions considered, showing the schematic view of the isotopes produced.

Here $f'(N)$ is the excess neutron binding energy to nuclei with a specified N over that given by the smooth Weizsacker mass formula normalised to zero at the beginning of the shell in which N lies. We have used the mass tables of Audi *et al.* (2003) and for various N, the resulting average values have been plotted against N. Another form of averaging is then affected by drawing a smooth curve through the points obtained in this way and plotted in Fig. 1. These equations are then solved for fixed values of Z, to obtain the corresponding values of A by trial and error, at different temperature and density conditions which specify Q_n in equation (8). The neutron capture paths so obtained are then plotted in Fig. 2.

5. Existence of chemical elements along the r-process path

In our classical condition we notice an element of mass 273 corresponding to atomic number 115. Experimentally some new elements were synthesized at the Lawrence Berkley Laboratory, e.g., elements with $Z = 116$, 118, etc. (Swiatecki *et al.* 2005). Also theories have long predicted the island of stability for nuclei with approximately 114 protons and 184 neutrons. Thus we conclude that a nuclei with mass 273 is a possibility. The seed nuclei in the neutrino driven wind are produced early in the expansion by alpha-capture or by proton-capture processes. When the temperature and density become low in a short dynamic time scale and the charged particle reactions almost cease, the r-process starts from these seed nuclei. So we start our calculation at ${}_{20}\mathrm{Ca}^{40}$ and obtain the neutron capture path beyond that.

We notice that at densities $>10^{30}\,\mathrm{cm}^{-3}$, the r-process chain does not show the elements as seen in data of Audi *et al.* (2003). As we try to obtain the elements at lower densities in our analysis, we find them more prominently as we go from high to low density site. Most of our observed elements are seen in the range of neutron number density $10^{20}\,\mathrm{cm}^{-3}$ to $10^{24}\,\mathrm{cm}^{-3}$ and temperature from 2.0×10^9 K to 3.0×10^9 K. For example, at densities $10^{28}\,\mathrm{cm}^{-3}$, $10^{26}\,\mathrm{cm}^{-3}$, etc., the r-process chain does not give us all the observable elements. But at condition of density $10^{20}\,\mathrm{cm}^{-3}$ and temperature $T_9 = 2.0$, that path contains all the elements as was given in the experimental data of Audi *et al.* (2003).

We tabulate some of the elements (experimental) obtained along the r-process path as follows:

We note that the element ${}_{98}\mathrm{Cf}^{254}$ shown by the supernova light curves is found in our classical astrophysical condition of temperature $T_9 = 1.9$ and neutron number density $n_n = 10^{20}\,\mathrm{cm}^{-3}$. We also note that the double magic nucleus ${}_{28}\mathrm{Ni}^{78}_{50}$ is obtained at $T_9 = 1.0$ and $n_n = 10^{20}\,\mathrm{cm}^{-3}$; $T_9 = 1.1$ and $n_n = 10^{22}\,\mathrm{cm}^{-3}$; $T_9 = 1.2$ and $n_n = 10^{24}\,\mathrm{cm}^{-3}$; $T_9 = 1.4$ and $n_n = 10^{26}\,\mathrm{cm}^{-3}$; $T_9 = 2.0$ and $n_n = 10^{28}\,\mathrm{cm}^{-3}$; all of these conditions correspond to Q_n value ≈ 2.5 Mev. Another double magic

Table 2. Chemical elements at the r-process site.

Element	$T_9(10^9\,\mathrm{K})$	$n_n(\mathrm{cm}^{-3})$
${}_{56}\mathrm{Ba}^{137}$	2.5	10^{20}
${}_{82}\mathrm{Pb}^{207}$	2.5	10^{22}
${}_{92}\mathrm{U}^{236}$	3.0	10^{22}
${}_{98}\mathrm{Cf}^{254}$	1.9	10^{20}
For double magic nuclei		
${}_{28}\mathrm{Ni}^{78}_{50}$	1.0	10^{20}
	1.1	10^{22}
	1.2	10^{24}
	1.4	10^{26}
	2.0	10^{28}
${}_{50}\mathrm{Sn}^{132}_{82}$	1.7	10^{20}
	1.9	10^{22}

nucleus ${}_{50}\mathrm{Sn}_{82}^{132}$ is found in our analysis at $T_9 = 1.7$ and $n_n = 10^{20}\,\mathrm{cm}^{-3}$; $T_9 = 1.9$ and $n_n = 10^{22}\,\mathrm{cm}^{-3}$; these correspond to Q_n value ≈ 4.5 Mev.

6. Discussion and conclusion

Whenever and however the r-process operates, it appears to be very uniform and well confined in astrophysical parameter space. The temperature, density and neutron flux at r-process sites vary over a small range. This means that only a small minority of type II supernovae produces r-process elements. The beta decay lifetimes, separation energy, neutron flux, the temperature range, the equilibrium chain and collapse time, all are built in to the equations, which are, then numerically solved to determine the chain for various separation energies. The neutrino winds drive out the r-process elements which then decay to the lines nearer to the beta-stable valley, and, they are ready for comparison with observation.

We have studied the r-process path at various temperatures ranging from 1.0×10^9 K to 3.0×10^9 K and neutron number densities ranging from $10^{20}\,\mathrm{cm}^{-3}$ to $10^{30}\,\mathrm{cm}^{-3}$. We mostly concentrate our analysis at energies greater than 2 Mev as this is the condition prevailing in the supernova envelopes and neutron capture occurs during the later expanding stage. We have used the mass table of Audi *et al.* (2003) for the calculation of the average excess neutron binding energy which is obtained by the normalization at the magic neutron numbers 20, 50, 82, 126. It has been found that a nucleus is stable if the number of neutrons or protons in it is equal to the magic number, and it cannot capture further neutrons because the shells are closed and they cannot contain an extra neutron. With the subsequent addition of neutrons at fixed Z, correspondingly the binding falls and ultimately falls to zero. At this point, the nucleus undergoes a β-decay and gets converted to the next element. This r-process path is shown in Fig. 2 by corresponding relations between Z and A.

As the high density conditions do not show much of the experimentally observed elements, we propose that the heavy elements which must have been produced during the extreme condition of supernova explosion instantly undergo photo-disintegration at the high density and temperature situation. Only in the later expansion stages after the explosion, where the neutron density supposedly falls, the r-process nucleosynthesis produces the heavy elements which subsequently β-decays and the r-process path forms. We conclude that the heavy elements were created after supernova explosion and in the later expansion stages they were distributed all over the universe. In supernova during the expansion stage if the ejected matter flow reaches the waiting point nuclei associated with the magic neutron numbers at rather small radii above the neutron star, neutrino induced charged current reactions can compete with the β-decays of the longest lived waiting point nuclei and thus speed up the matter flow to heavier nuclei. We tried to get our abundances with respect to all the nuclei whose β-decay lifetimes are considerably higher. We conclude that our theoretical model will be successful in providing new light to solve some problems in the r-process and the corresponding build-up to heavier nuclei.

Acknowledgements

The authors are sincerely thankful to the Government of Assam for giving the permission to carry out the research work. Grateful thanks are due to B. K. Rajkhowa of

POWIET and Dr S. M. Hazarika of Tezpur University for their valuable help during the preparation of the manuscript.

References

Arnett, W. D. 1979, Proceedings of the workshop on Sources of Gravitational Radiation, Cambridge University Press, 311.
Audi, G., Wapstra, A. H., Thibault, C. 2003, *Nucl. Phys. A*, **729**, 337.
Borzov, I. N., Goriely, S. 2000, *Phys. Rev. C*, **62**, 03550.
Bruenn, S. W. 1989a, *ApJ*, **340**, 955.
Burbidge, E. M., Burbidge, G. R., Fowler, W. A., Hoyle, F. 1957, *Rev. Mod. Phys.*, **29**, 547.
Chetia, A., Duorah, H. L. 1986, *Il Nuovo Cimento*, **94B**, 93.
Fermi, E. 1950, University of Chicago, Chicago I11, 8.
Freiburghaus, C., Rembges, J. F., Rauscher, T., Kolbe, E., Thielemann, F. K., Kratz, K. L., Pfeiffer, B., Cowan, J. J. 1999, *ApJ*, **516**, 381.
Janka, H. T. 1993, Frontier Objects in Astrophysics and Particle Physics (eds) Giovannelli, F., Mannocchi, G., *Conf. Proc., SIF, Bologna*, **40**, p345.
Kratz, K. L., Pfeiffer, B., Thielemann, F. K., Bitouzet, J. P., Moller, P. 1993, *ApJ*, **402**, 216.
Mathews, G. J., Cowan, J. J. 1992, *ApJ*, **391**, 719.
Meyer, B. S., Mathews, G. J., Howard, W. M., Woosley, S. E., Hoffman, R. D. 1992, *ApJ*, **399**, 656.
Mukhopadhyay, B. 2007, *Class. Quant. Grav.*, **24**, 1433.
Qian, Y. Z., Vogel, P., Wasserburg, G. J. 1998, *ApJ*, **494**, 285.
Schramm, D. N. 1973, Proceedings of Conference on Explosive Nucleosynthesis, Austin, Texas.
Swiategki, W. J., Wilczynska, K. S., Wilczynski, J. 2005, *Phys. Rev. C.*, **71**, 014602.
Takahashi, K., Witti, J., Janka, H. T. 1994, *A&A*, **286**, 857.
Terasawa, M., Sumiyoshi, K., Kajino, T., Mathews, G. J., Tanihata, I. 2001, *ApJ*, **562**, 470.
Wanajo, S., Tamamura, M., Itoh, N., Nomoto, K., Ishimaru, Y., Beers, T. C., Nozawa, S. 2003, *ApJ*, **593**, 968.
Wilson, J. R., Mayle, R. W., Woosley, S. E., Weaver, T. 1986, *Ann. N. Y. Acad. Sci.*, **470**, 267.
Witti, J., Janka, H. T., Takahashi, K. 1994, *A&A*, **286**, 841.
Woosley, S. E., Hoffman, R. D., 1992, *ApJ*, **395**, 202.
Woosely, S. E., Wilson, J. R., Mathews, G. J., Hoffman, R. D., Meyer, B. S. 1994, *ApJ*, **433**, 229.